Valence-Shell Autoionization of NO

S.H. Southworth, T.A. Ferrett, J.E. Hardis, A.C. Parr, and J.L. Dehmer

Abstract

Autoionization of valence and Rydberg states in NO over the 12.5–18 eV photon energy range was studied by vibrationally resolved photoelectron spectroscopy of the 2 π orbital. Complex, oscillatory structure is observed in NO^+ ($2\pi^{-1}$) $X^1\Sigma^+$ partial cross sections, branching ratios, and photoelectron anisotropy parameters due to autoionizing valence states and Rydberg states associated with the $1\pi^{-1}$ and $5\sigma^{-1}$ channels. Autoionization of the $5\sigma \rightarrow np(\pi, \sigma)$ ($v' = 0$), n = 3–5 Rydberg states leading to the ($5\sigma^{-1}$) $b^3\Pi$ state of NO^+ produces very high vibrational levels of ($2\pi^{-1}$) $X^1\Sigma^+$. Autoionization of the $5\sigma \rightarrow 3p\pi$ ($v' = 0$) Rydberg state was characterized by resonance profiles of photoelectron cross sections and angular distributions.

Key words: molecular autoionization, photoelectron spectroscopy, synchrotron radiation

1. INTRODUCTION

One of Professor Ugo Fano's enduring and influential contributions to our understanding of physical principles is the elucidation of resonances in ionization continua. His work in the early 1960s on the configuration-interaction model of autoionizing resonances provided a general approach to treating resonant ionization phenomena.[1] That work coincided with early developments of synchrotron-radiation sources for spectroscopy, particularly for studies of autoionizing resonances in atomic photoabsorption spectra.[2] The basic idea of quasi-bound states interacting with ionization continua has been extensively expanded upon and refined by Fano and his students and collaborators, and has inspired many others to contribute to the understanding of various aspects of this basic process. Theoretical developments have gone hand in hand with the development of increasingly sensitive experimental methods, such as intense, high-resolution, synchrotron-radiation beam-lines combined with high-resolution, angle-resolved photoelectron spectrometers. The ability to measure photoionization cross sections' differentials with respect to angle and final state as continuous functions of photon energy allows critical testing of theory.

Within the broad field of photoionization research, the study of molecular valence electrons has attracted much attention. Fano and coworkers made fundamental contributions to the understanding of molecular photoionization.[3–5] Uniquely molecular aspects of resonant photoionization can be studied by vibrationally resolved photoelectron spectroscopy. Resonances in photoionization continua arising from potential barriers (shape resonances) and many-electron interactions (bound-continuum and continuum-continuum) are manifested in photoelectron cross sections, branching ratios, and angular distributions.[6] The study of "molecular photoelectron dynamics" is quite challenging for both experiment and theory. On the experimental side, intense and continuously tunable photon sources with angle-resolved, high-resolution photoelectron spectrometers are required. On the theoretical side, the powerful calculational methods that have been so successful in describing atomic photoionization cannot readily be applied to molecules because of their nonspherical geometries and large number of degrees of freedom.

In this paper, we illustrate some aspects of valence-shell resonant photoionization of molecules by presenting results of a photoelectron spectroscopy study of the 2 π orbital of NO using tunable synchrotron radiation. Several experimental[7–22] and theoretical[23–32] studies of NO^+ ($2\pi^{-1}$) have been reported. (We exclude laser-based studies from the present discussion.[33]) A major thrust of early studies was the search for broad, shape-resonant features at the electronically resolved level.[12–14,23–26,28] Subsequent studies demonstrated vibrationally dependent photoelectron branching ratios and anisotropies, but with coarse photon-energy steps in the experiment[15] and single-electron treatment in the theory.[31] An ongoing challenge for theory is the treatment of many-electron interactions, which appear in experimental spectra as sharp features due to bound-continuum interactions or broad features due to continuum-continuum interactions. Various theoretical approaches have been reported on Rydberg autoionizing states and Rydberg-valence mixed autoionizing states.[20,26,27,29,30,32] In the experimental study described here, the photon-energy step size was small enough to clearly reveal autoionizing structure in the photoelectron cross sections, branching ratios, and anisotropies. Selected results will be discussed to illustrate how resonances are manifested in molecular photoelectron spectra.

The molecular-orbital configuration of ground-state NO is $1\sigma^2 2\sigma^2 3\sigma^2 4\sigma^2 5\sigma^2 1\pi^4 2\pi$, $X^2\Pi$. The open-shell structure gives

rise to a complex valence photoelectron spectrum over 9–25 eV binding energy from the 2π, 1π, 5σ, and 4σ orbitals and correspondingly complex sets of Rydberg series in the photoabsorption spectrum.[8,18–20] The antibonding 2π electron has a relatively low binding energy of 9.264 eV, corresponding to the $v^+ = 0$ vibrational level of the ground ionic state NO^+ $(2\pi^{-1})$ $X^1\Sigma^+$.[34] A wide gap of binding energy is available for recording high vibrational levels of $2\pi^{-1}$ in the photoelectron spectrum before the appearance of the second electronic state, $(1\pi^{-1})$ $a^3\Sigma^+$, at 15.67 eV. While only the $v^+ = 0$–5 vibrational levels of $2\pi^{-1}$ are significantly populated in a direct photoionization process, due to the Franck–Condon factors,[35] very high vibrational levels were observed in early photoelectron spectra recorded using discrete-line photon sources whose energies coincided with autoionizing Rydberg states.[9–11] With intense, tunable, synchrotron-radiation sources, photoelectron spectra can be recorded as continuous functions of photon energy to enable more complete studies of resonant photoionization. Here we present partial results of experiments in which vibrationally resolved photoelectron cross sections, branching ratios, and anisotropies were determined for NO^+ $(2\pi^{-1})$ $X^1\Sigma^+$. First, the $v^+ = 0$–5 levels (the "Franck–Condon band") were measured over $h\nu = 12.5$–18 eV with 0.01 eV steps and 2 Å bandwidth to map out resonance structure over a broad energy range. Second, all energetically allowed vibrational levels were recorded on the autoionizing Rydberg resonances $5\sigma \rightarrow 3p\pi$ $(v' = 0)$, $5\sigma \rightarrow 4p(\pi, \sigma)$ $(v' = 0)$, and $5\sigma \rightarrow 5p(\pi, \sigma)$ $(v' = 0)$ associated with the $(5\sigma^{-1})$ $b^3\Pi$ state of NO^+. Third, the $v^+ =$ 0–16 levels were measured through the $5\sigma \rightarrow 3p\pi$ $(v' = 0)$ Rydberg resonance with 0.7 Å bandwidth to determine resonance profiles of partial cross sections and anisotropies. Photoelectron spectroscopy studies with results similar to those discussed here have been reported by Mitsuke et al.[21] and Salzmann et al.,[22] and unpublished spectra were recorded by Cafolla et al.[16] and Roy and Krause.[17]

2. EXPERIMENTAL METHODS

Measurements were made at the Synchrotron Ultraviolet Radiation Facility at the National Institute of Standards and Technology on the 2 m normal-incidence-monochromator beam-line.[36] A glass capillary channeled the radiation from the monochromator exit slit into the spectrometer chamber and acted as an effective gas-conduction barrier. The photon flux was measured by calibrated tungsten photoemissive photodiodes.[37] The beam-line was operated without an entrance slit, and the bandwidth was adjustable between 0.7 and 2.0 Å (FWHM) by adjusting the vertical size of the stored electron bunch.

For randomly oriented target molecules, the differential photoionization cross section in the electric-dipole approximation can be expressed as[38]

$$\frac{d\sigma}{d\Omega} = \frac{\sigma}{4\pi}\left[1 + \frac{\beta}{4}(1 + 3p\cos 2\theta)\right], \qquad (1)$$

where σ is the angle-integrated cross section, β is the photoelectron anisotropy parameter, p is the degree of linear polarization of the photon beam, and θ is the angle of photoelectron emission with respect to the major axis of the polarization ellipse. The parameters σ and β are determined by the photoionization transition amplitudes and vary with energy in response to resonances.[5] The goal of the experiment was to determine σ and β for each vibrational level of NO^+ $(2\pi^{-1})$ $X^1\Sigma^+$ as functions of photon energy. The photoelectron spectrometer features two hemispherical electron analyzers positioned in the plane perpendicular to the photon beam. One analyzer is fixed at $\theta = 0°$ and the other is rotatable over $\theta \approx 0° - 90°$, but the rotatable analyzer was fixed at $\theta = 90°$ for this experiment. The spectrometer system was essentially as described in Ref. 39, except the channeltrons were replaced with microchannel plates and resistive-anode encoders (MCP-RAE) for simultaneous recording of a range of kinetic energies. In the data collection procedure, the potentials on the analyzers were varied so that each kinetic energy was recorded at each position of the MCP-RAE to eliminate variations of detection efficiency with position. The relative collection efficiencies of the 0° and 90° analyzers with respect to kinetic energy were determined by measurements of Ar 3p photoelectrons, for which σ[40] and β[41] are known fairly well. The degree of linear polarization of the photon beam was measured with a triple-reflection polarizer[42] attached to the rotatable analyzer and was determined to be $p = 0.65(3)$ for photon energies below 20 eV.

The photoelectron spectra were corrected for the relative collection efficiencies of the analyzers, and fitting procedures were used to obtain peak areas for each vibrational level in the 0° and 90° spectra. The areas were normalized with respect to photon flux and sample-gas density. The normalized areas were then used in (1) to determine relative partial cross sections, anisotropy parameters, and vibrational branching ratios.

3. RESULTS AND DISCUSSION

In a direct photoionization process, the relative intensities of vibrational levels produced in the molecular ion are largely determined by the squares of the overlap integrals between the ground-state and ionic-state vibrational wave-functions, i.e., the Franck–Condon factors. For NO^+ $(2\pi^{-1})$ $X^1\Sigma^+$, the Franck–Condon factors are significant ($\geq 1\%$) for the $v^+ =$ 0–5 levels.[35] To obtain an overview of resonance structure in the $2\pi^{-1}$ channel, the $v^+ = 0$–5 levels were measured over $h\nu = 12.5$–18 eV with 0.01 eV steps and 2 Å bandwidth. The vibrationally summed cross section is plotted in Fig. 1 and on an expanded scale in Fig. 2 along with the vibrationally averaged anisotropy parameter β. Autoionization of Rydberg states associated with the $1\pi^{-1}$ and $5\sigma^{-1}$ channels produces structure in the $2\pi^{-1}$ cross section throughout this photon-energy range. Some of the resonant features are identified in Fig. 1, based on recent analysis of the photoabsorption spectrum by Erman et al.[18–20] Autoionization of both

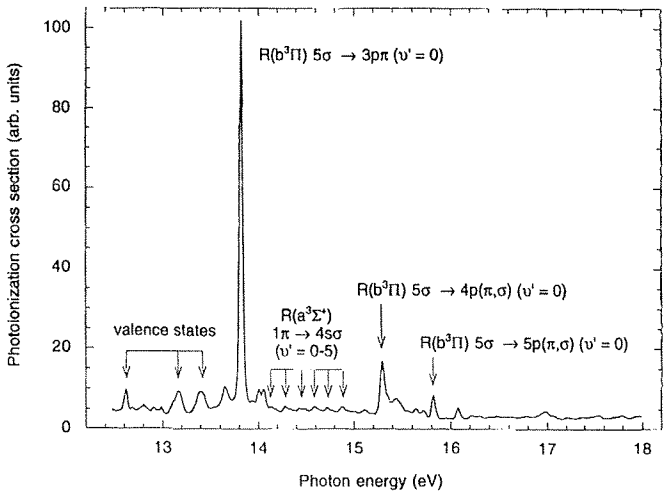

Figure 1. Relative photoionization cross section summed over the $v^+ = 0$–5 vibrational levels of NO^+ $(2\pi^{-1})$ $X^1\Sigma^+$. Some of the structure in the cross section is assigned to autoionizing valence states and Rydberg states, based on analysis of the photoabsorption spectrum by Erman et al.[18–20]

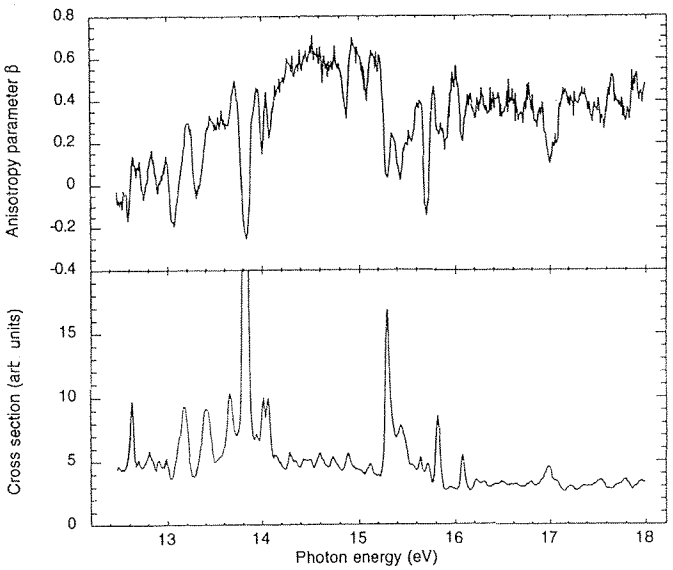

Figure 2. Top: vibrationally averaged anisotropy parameter β for the $v^+ = 0$–5 vibrational levels of NO^+ $(2\pi^{-1})$ $X^1\Sigma^+$. Bottom: relative photoionization cross section summed over the $v^+ = 0$–5 vibrational levels of NO^+ $(2\pi^{-1})$ $X^1\Sigma^+$ (same data as in Fig. 1).

Rydberg states and valence states is observed. The β parameter is quite sensitive to the resonances, as expected based on theoretical considerations of the relation between β and transition amplitudes.[5] Comparing the response of β with corresponding peaks in the cross section, the β parameter tends to oscillate through minima. Oscillatory behavior of cross sections and angular distributions is characteristic of autoionization processes.[1,5,43,44] Complex structure in σ and β could not be clearly observed in previous experimental studies of NO^+ $(2\pi^{-1})$ made with coarse photon-energy steps.[13,15] Data over a wide photon-energy range are useful to test and develop molecular photoionization theory for specific treatments of correlated wave-functions, shape resonances, and autoionizing Rydberg and valence states.[23–32] The vibrationally resolved σ and β results for the $v^+ = 0$–5 levels show significant vibrational dependencies, which can be attributed, in part, to the dependence of transition amplitudes on internuclear separation.[6,31] Those results will be discussed in a full report elsewhere.

The most intense autoionizing resonances observed in the $2\pi^{-1}$ cross section are due to the Rydberg states $5\sigma \rightarrow 3p\pi$ $(v' = 0)$, $5\sigma \rightarrow 4p(\pi, \sigma)$ $(v' = 0)$, and $5\sigma \rightarrow 5p(\pi, \sigma)$ $(v' = 0)$ leading to the $(5\sigma^{-1})$ $b^3\Pi$ state of NO^+. The $2\pi^{-1}$ photoelectron spectra recorded with the 0° analyzer at the peaks of those resonances with 0.7 Å bandwidth are plotted in Fig. 3. Essentially all energetically accessible vibrational levels of $(2\pi^{-1})$ $X^1\Sigma^+$ are produced with significant intensities at each resonance. The vibrational branching ratios and anisotropy parameters are plotted in Figs. 4 and 5. One or two of the highest vibrational levels, those with kinetic energies below 0.3 eV, were excluded from the data analysis, because the collection efficiencies determined for our electron analyzers are uncertain below 0.3 eV. The branching ratios show that while the lower vibrational levels remain strongly populated, as in a direct ionization process, secondary maxima appear in the intensities of the higher vibrational levels. The β values also show considerable variations among the vibrational levels.

Understanding resonant variations of partial cross sections, branching ratios, and angular distributions requires theoretical developments beyond those of Fano and Cooper.[1] Mies[45] extended Fano's theory to treat the interaction of many resonances with many continua in order to apply the theory to molecular processes. In the present case, the $5\sigma \rightarrow 3p\pi$ $(v' = 0)$ resonance at 13.82 eV is strong compared with other nearby Rydberg states and might be treated as an isolated resonance if its unresolved rotational structure is ignored. The ion-continuum channels to which it decays consist of the $v^+ = 0$–17 levels of NO^+ $(2\pi^{-1})$ $X^1\Sigma^+$, since higher electronic states of NO^+ are closed at this photon energy. The $(2\pi^{-1})$ $X^1\Sigma^+$ state is also the only open electronic state of NO^+ at the energy of the $5\sigma \rightarrow 4p(\pi, \sigma)$ $(v' = 0)$ resonance, while the $v^+ = 0$ and 1 levels of the $(1\pi^{-1})$ $a^3\Sigma^+$ state (not plotted in Fig. 3) are also open at the energy of the $5\sigma \rightarrow 5p(\pi, \sigma)$ $(v' = 0)$ resonance.

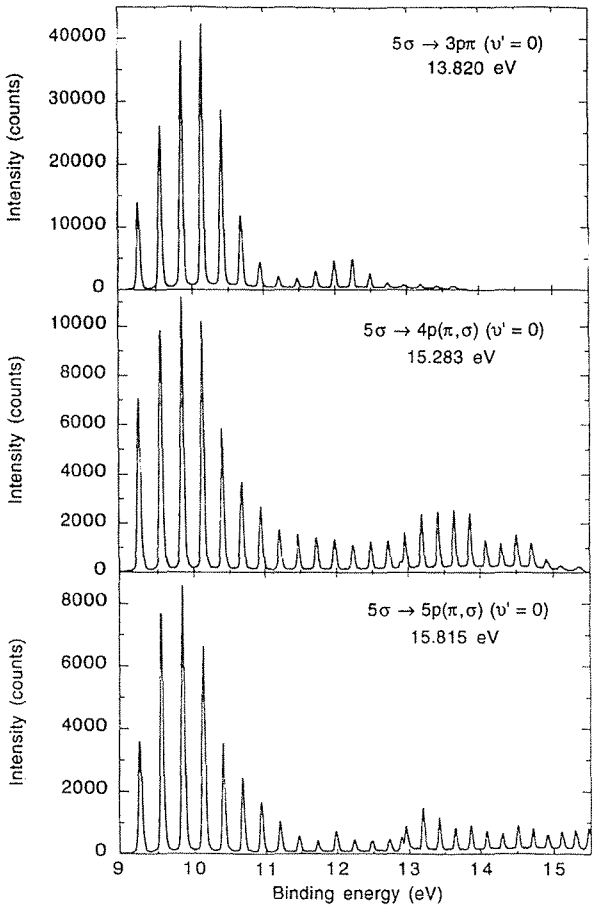

Figure 3. Photoelectron spectra of NO^+ $(2\pi^{-1})$ $X^1\Sigma^+$ recorded at the peaks of Rydberg resonances. Top: $5\sigma \rightarrow 3p\pi$ $(v' = 0)$; middle: $5\sigma \rightarrow 4p(\pi, \sigma)$ $(v' = 0)$; bottom: $5\sigma \rightarrow 5p(\pi, \sigma)$ $(v' = 0)$.

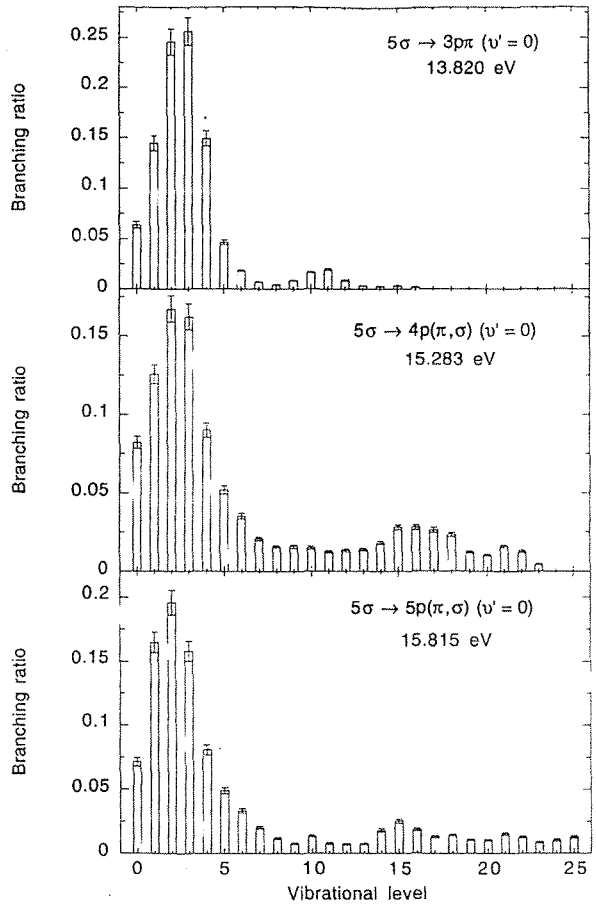

Figure 4. Vibrational branching ratios for NO^+ $(2\pi^{-1})$ $X^1\Sigma^+$ measured at the peaks of Rydberg resonances. Top: $5\sigma \rightarrow 3p\pi$ $(v' = 0)$; middle: $5\sigma \rightarrow 4p(\pi, \sigma)$ $(v' = 0)$; bottom: $5\sigma \rightarrow 5p(\pi, \sigma)$ $(v' = 0)$.

Starace[43] developed the theoretical forms of resonant variations of partial cross sections and branching ratios, and Kabachnik and Sazhina[44] developed the resonant forms of photoelectron angular distributions and polarizations. To understand the vibrational distribution produced in a molecular ion in an autoionization process, Bardsley[46] assumed that the Born–Oppenheimer separation of electronic and nuclear motion is valid and concluded that the Franck–Condon factors between the Rydberg state and the ionic state would be important. This idea was confirmed by Berkowitz and Chupka,[47] who used a retarding-field analyzer to make one of the first photoelectron studies of molecular autoionization. Smith[48] used Mies's[45] extension of the Fano theory to derive expressions for vibrational intensities in terms of Franck–Condon factors among the ground state, quasi-bound excited state, and ionic state along with the q and ε parameters from the Fano formulation.[1] An example of the application of the Smith model to autoionization in O_2 was described by Eland.[49]

Within the Smith model, molecular autoionization is described by vibronic transitions among the potential curves of the ground state, Rydberg state, and ionic state. The vibrational branching ratios measured in the photoelectron spectrum can be used to infer the potential-curve parameters of the quasi-bound Rydberg state.[46–49] Such an analysis, however, makes no use of information contained in the β parameters.

A major development beyond the configuration-interaction treatments of autoionizing resonances has been multichannel quantum-defect theory (MQDT),[50] the origins of which are credited to Seaton[51] and Fano.[4] The MQDT treats interactions among entire Rydberg series and continuum channels comprehensively and is well suited to deriving the complex structures observed in photoelectron cross sections, branching ratios, and anisotropies over wide photon-energy ranges. A good example is the MQDT calculation of Leyh and Raseev[52] on valence-shell autoionization

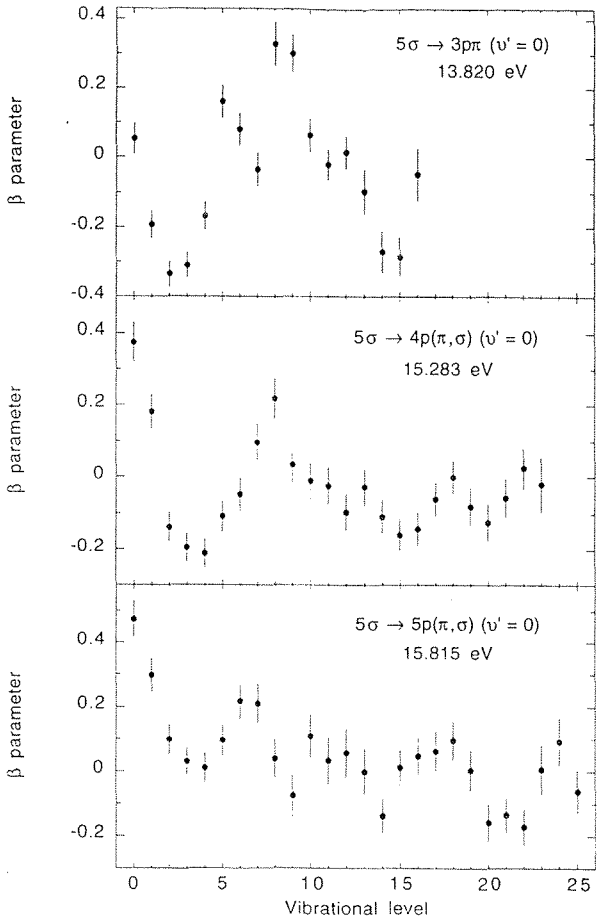

Figure 5. Anisotropy parameters for NO^+ $(2\pi^{-1})$ $X^1\Sigma^+$ measured at the peaks of Rydberg resonances. Top: $5\sigma \rightarrow 3p\pi$ $(v' = 0)$; middle: $5\sigma \rightarrow 4p(\pi, \sigma)$ $(v' = 0)$; bottom: $5\sigma \rightarrow 5p(\pi, \sigma)$ $(v' = 0)$.

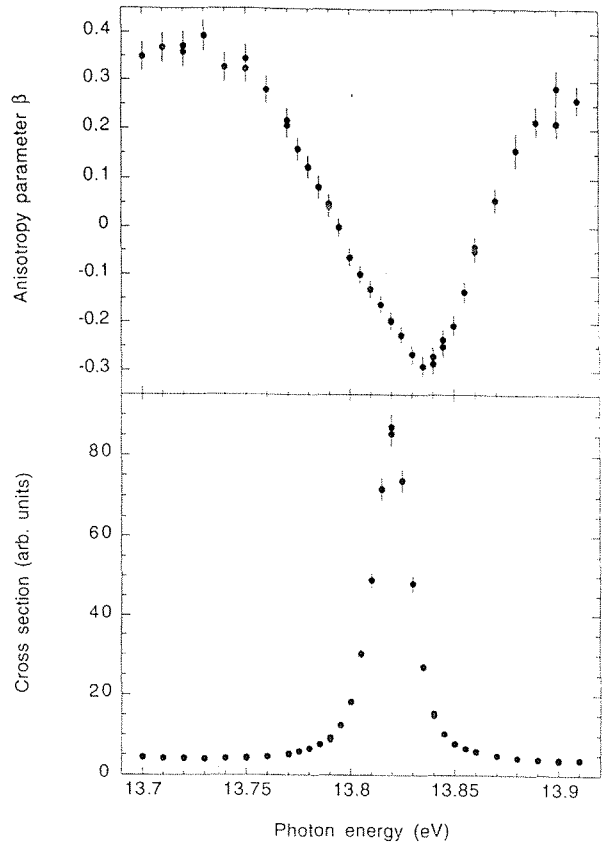

Figure 6. Photoelectron cross section and anisotropy profiles of NO^+ $(2\pi^{-1})$ $X^1\Sigma^+$ measured through the $5\sigma \rightarrow 3p\pi$ $(v' = 0)$ Rydberg resonance. Top: vibrationally averaged anisotropy parameter for the $v^+ = 0$–16 vibrational levels. Bottom: relative photoionization cross section summed over the $v^+ = 0$–16 vibrational levels.

dynamics of CO and its comparison with the vibrationally and angularly resolved photoelectron data of Hardis et al.[53] using the same instrumentation as in the present study of NO. The CO study[53] found qualitative agreement between theory and experiment for the resonance behavior of vibrational branching ratios but major discrepancies for the β parameters. That result emphasizes the sensitivity of β to interference among transition amplitudes[5] and, hence, its value in testing theory.

We present a final example here in the case of NO^+ $(2\pi^{-1})$. To more completely characterize autoionization of the $5\sigma \rightarrow 3p\pi$ $(v' = 0)$ resonance at 13.82 eV, the $v^+ = 0$–16 levels were measured across the resonance region with small photon-energy steps and 0.7 Å bandwidth. The vibrationally averaged σ and β are shown in Fig. 6. While the resonance in the cross section is nearly symmetric, the feature in β is much broader and asymmetric. Space limitations preclude a presentation here of the variations with v^+ that are observed in the vibrationally resolved σ and β. We expect these data will provide an interesting problem for theoretical studies of molecular autoionization.

There is an additional decay mode available to molecules in response to resonant excitation, namely, dissociation into neutral fragments. Predissociation competes with preionization in the decay of resonances that lie energetically above both dissociative and ionization thresholds. The neutral-dissociation threshold of NO is at 6.496 eV, well below the ionization threshold of 9.264 eV.[34] The quantum yield of ionization of NO is approximately 42% at the $5\sigma \rightarrow 3p\pi$ $(v' = 0)$ resonance at 13.82 eV.[7] Assuming that molecular fluorescence is relatively weak, the quantum-yield data show that both predissociation and preionization are strong processes. Giusti-Suzor and Jungen[27] have used MQDT to study competition between vibrational preionization and electronic predissociation in NO at lower photon energies where Rydberg-valence state interaction is important. Competition between ionization and dissociation is clearly

occurring in the present case of electronic autoionization of NO. Whether or not there is a significant interaction that is reflected in the vibrationally dependent resonant profiles of σ and β might be an interesting question for theory to address.[54]

In conclusion, results were presented from an angle-resolved and vibrationally resolved photoelectron study of valence-shell autoionization of NO. Small photon-energy steps were used to observe complex oscillatory structures in NO^+ $(2\pi^{-1})$ $X^1\Sigma^+$ cross sections and anisotropy parameters due to autoionizing Rydberg and valence-excited states. Very high vibrational levels of the molecular ion were produced by autoionizing Rydberg resonances. The study of molecular photoelectron dynamics has progressed due to improved instrumentation and the development of increasingly accurate theoretical models. However, much work remains to be done before molecular autoionization can be considered satisfactorily understood, and we hope that the present results on NO will contribute to that effort.

Acknowledgments

We are grateful to the staff at SURF for their support during the course of this work. S.H.S. was supported by the U.S. Department of Energy, Office of Basic Energy Sciences, Division of Chemical Sciences, under Contract No. W-31-109-Eng-38.

Received 19 June 2000.

Résumé

L'autoionisation des états de valence et de Rydberg de NO a été étudié par spectroscopie de photoélectrons résolue vibrationellement de l'état NO^+ $(2\pi^{-1})$ pour des énergies hv = 12.5–18 eV. Une structure complexe et oscillatoire due à l'autoionisation des états de valence et de Rydberg associés aux voies $1\pi^{-1}$ et $5\sigma^{-1}$ a été observée dans les sections efficaces partielles, les rapports de branchement, et les paramètres d'anisotropie de l'état NO^+ $X^1\Sigma^+$. L'autoionisation des états de Rydberg $5\sigma \rightarrow np(\pi,\sigma)$ $(v' = 0)$, $n = 3$–5, donnant lieu à l'état NO^+ $(5\sigma^{-1})$ $b^3\Pi$ produit les niveaux vibrationnels hautement excités de l'état $(2\pi^{-1})$ $X^1\Sigma^+$. L'autoionisation de l'état de Rydberg $5\sigma \rightarrow 3p\pi(v' = 0)$ a été caractérisé par le profil de résonnance des sections efficaces de photoionisation, et des distributions angulaires.

References

1. U. Fano, Phys. Rev. **124**, 1866 (1961); U. Fano and J.W. Cooper, Phys. Rev. A **137**, 1364 (1965).
2. R.P. Madden and K. Codling, Phys. Rev. Lett. **10**, 516 (1963).
3. H.D. Cohen and U. Fano, Phys. Rev. **150**, 30 (1966).
4. U. Fano, Phys. Rev. A **2**, 353 (1970); J. Opt. Soc. Am. **65**, 979 (1975).
5. U. Fano and D. Dill, Phys. Rev. A **6**, 185 (1972) and Phys. Rev. Lett. **29**, 1203 (1972); D. Dill, Phys. Rev. A **7**, 1976 (1973).
6. J.L. Dehmer, A.C. Parr, and S.H. Southworth, in *Handbook on Synchrotron Radiation*, Vol. 2, edited by G.V. Marr (North-Holland, New York, 1987), pp. 241–353.
7. K. Watanabe, F.M. Matsunaga, and H. Sakai, Appl. Opt. **6**, 391 (1967).
8. O. Edqvist, E. Lindholm, L.E. Selin, H. Sjögren, and L. Åsbrink, Ark. Fys. **40**, 439 (1970); O. Edqvist, L. Åsbrink, and E. Lindholm, Z. Naturforsch. Teil A **26**, 1407 (1971).
9. V.I. Kleimenov, Yu.V. Chizhov, and F.I. Vilesov, Opt. Spectrosc. (USSR) **32**, 371 (1972).
10. J.L. Gardner and J.A.R. Samson, J. Electron Spectrosc. **2**, 153 (1973).
11. P. Natalis, J. Delwiche, J.E. Collin, G. Caprace, and M.-T. Praet, Chem. Phys. Lett. **49**, 177 (1977).
12. C.E. Brion and K.H. Tan, J. Electron Spectrosc. **23**, 1 (1981).
13. S. Southworth, C.M. Truesdale, P.H. Kobrin, D.W. Lindle, W.D. Brewer, and D.A. Shirley, J. Chem. Phys. **76**, 143 (1982).
14. Y. Iida, F. Carnovale, S. Daviel, and C.E. Brion, Chem. Phys. **105**, 211 (1986).
15. S.H. Southworth, A.C. Parr, J.E. Hardis, and J.L. Dehmer, J. Chem. Phys. **87**, 5125 (1987).
16. T. Cafolla, T. Reddish, and J. Comer, in *Proceedings of the 15th International Conference of Electronic and Atomic Collisions*, edited by J. Geddes, H.B. Gilbody, A.E. Kingston, C.J. Latimer, and H.J.R. Walters, abstract of contributed papers, 54 (1987).
17. P. Roy and M.O. Krause, unpublished.
18. P. Erman, A. Karawajczyk, E. Rachlew-Källne, and C. Strömholm, J. Chem. Phys. **102**, 3064 (1995).
19. P. Erman, A. Karawajczyk, E. Rachlew-Källne, E. Mevel, R. Zerne, A. L'Huillier, and C.-G. Walhström, Chem. Phys. Lett. **239**, 6 (1995).
20. P. Erman, A. Karawajczyk, E. Rachlew-Källne, M. Stankiewicz, K. Yoshiki Franzén, P. Sannes, and L. Veseth, Chem. Phys. Lett. **273**, 239 (1997).
21. K. Mitsuke, Y. Hikosaka, T. Hikida, and H. Hattori, J. Electron Spectrosc. **79**, 395 (1996).
22. M. Salzmann, M. Müller, N. Böwering, and U. Heinzmann, J. Phys. B **32**, 2517 (1999).
23. S. Wallace, D. Dill, and J.L. Dehmer, J. Chem. Phys. **76**, 1217 (1982).

24. J.J. Delaney, I.H. Hillier, and V.R. Saunders, J. Phys. B **15**, 1477 (1982).
25. M.E. Smith, R.R. Lucchese, and V. McKoy, J. Chem. Phys. **79**, 1360 (1983).
26. L.A. Collins and B.I. Schneider, Phys. Rev. A **29**, 1695 (1984).
27. A. Giusti-Suzor and Ch. Jungen, J. Chem. Phys. **80**, 986 (1984).
28. M.R. Hermann, C.W. Bauschlicher, Jr., W.M. Huo, S.R. Langhoff, and P.W. Langhoff, Chem. Phys. **109**, 1 (1986).
29. A.L. Sobolewski, J. Chem. Phys. **87**, 331 (1987).
30. D.L. Lynch, B.I. Schneider, and L.A. Collins, Phys. Rev. A **38**, 4927 (1988).
31. D.L. Lynch, B.I. Schneider, L.A. Collins, V. McKoy, and W.M. Huo, Chem. Phys. Lett. **147**, 529 (1988).
32. R.E. Stratmann, R.W. Zurales, and R.R. Lucchese, J. Chem. Phys. **104**, 8989 (1996).
33. K.S. Wang and V. McKoy, Ann. Rev. Phys. Chem. **46**, 275 (1995).
34. K.P. Huber and G. Herzberg, *Constants of Diatomic Molecules* (Van Nostrand Reinhold, New York, 1979), p. 466.
35. M.E. Wacks, J. Chem. Phys. **41**, 930 (1964).
36. D.L. Ederer, B.E. Cole, and J.B. West, Nucl. Instrum. Methods **172**, 185 (1980).
37. L.R. Canfield, in *Vacuum Ultraviolet Spectroscopy II*, edited by J.A.R. Samson and D.L. Ederer (Academic Press, San Diego, 1998), pp. 117–138.
38. J.A.R. Samson and A.F. Starace, J. Phys. B **8**, 1806 (1975); Corrigendum **12**, 3993 (1979).
39. A.C. Parr, S.H. Southworth, J.L. Dehmer, and D.M.P. Holland, Nucl. Instrum. Methods Phys. Res. **222**, 221 (1984).
40. G.V. Marr and J.B. West, At. Data Nucl. Data Tables **18**, 497 (1976).
41. S.H. Southworth, A.C. Parr, J.E. Hardis, J.L. Dehmer, and D.M.P. Holland, Nucl. Instrum. Methods Phys. Res. A **246**, 782 (1986).
42. V.G. Horton, E.T. Arakawa, R.N. Hamm, and M.W. Williams, Appl. Opt. **8**, 667 (1969).
43. A.F. Starace, Phys. Rev. A **16**, 231 (1977).
44. N.M. Kabachnik and I.P. Sazhina, J. Phys. B **9**, 1681 (1976).
45. F.H. Mies, Phys. Rev. **175**, 164 (1968).
46. J.N. Bardsley, Chem. Phys. Lett. **2**, 329 (1968).
47. J. Berkowitz and W.A. Chupka, J. Chem. Phys. **51**, 2341 (1969).
48. A.L. Smith, Philos. Trans. R. Soc. London, Ser. A **268**, 169 (1970).
49. J.H.D. Eland, J. Chem. Phys. **72**, 6015 (1980).
50. C.H. Greene and Ch. Jungen, in *Advances in Atomic and Molecular Physics*, Vol. 21 (Academic Press, New York, 1985), p. 51.
51. M.J. Seaton, Proc. Phys. Soc. London **88**, 801 (1966).
52. B. Leyh and G. Raseev, J. Chem. Phys. **89**, 820 (1988).
53. J.E. Hardis, T.A. Ferrett, S.H. Southworth, A.C. Parr, P. Roy, J.L. Dehmer, P.M. Dehmer, and W.A. Chupka, J. Chem. Phys. **89**, 812 (1988).
54. Ch. Jungen and S.C. Ross, Phys. Rev. A **55**, R2503 (1997).

S.H. Southworth
Argonne National Laboratory
Argonne, Illinois 60439 U.S.A.

e-mail: southworth@anl.gov

T.A. Ferrett
Carleton College
Northfield, Minnesota 55057 U.S.A.

J.E. Hardis and A.C. Parr
National Institute of Standards and Technology
Gaithersburg, Maryland 20899 U.S.A.

J.L. Dehmer
National Science Foundation
Arlington, Virginia 22230 U.S.A.